Improvement of EV Maneuverability and Safety by Disturbance Observer Based Dynamic Force Distribution

PENG HE
Department of Electrical Engineering
The University of Tokyo
7-3-1 Hongo, Bunkyo-ku, Tokyo113-8654 Japan
E-mail: ka@horilab.iis.u-tokyo.ac.jp
YOICHI HORI
Institute of Industrial Science
The University of Tokyo
7-3-1 Hongo, Bunkyo-ku, Tokyo113-8654 Japan
E-mail: hori@iis.u-tokyo.ac.jp

Abstract

By optimally controlling EV in-wheel driving motors, traction forces between tire and road can be generated. Due to such precise traction force generation, yaw moment, which effects EV motion, can be controlled exactly. Yaw moment control improves maneuverability and keeps safety of EV, even in the case of acceleration or deceleration cornering.

First, in this paper, we analyze the characteristics of EV. Next, we design a reference model, which has an expected maneuverability characteristics, and also use it for model following control. Second, we design a disturbance observer to estimate the traction forces on the driving wheels and the yaw moment generated by those traction forces. Third, using the observer outputs, we design the optimum distribution controller for traction force control.

Using the proposed control methods, the required yaw moment is generated and controlled effectively, by which maneuverability and stability of EV can be improved to have almost the same characteristics as reference model. Simulations and experiments are to be performed to test the effectiveness of proposed control strategy.

Keywords: Controller, Control System, Wheel motor

1 Introduction

In recent years, considering environmental protection and energy conservation, researches for electric vehicle (EV) have been put forward greatly. In the middle of the 21st century, EV will be the major tool of transportation system.

In-wheel motored EV is looked on as a new developed one. The typical configurations of that EV are in wheel motors, which are installed into wheels and can be controlled independently [1] [2]. Figure 1 shows our EV whose name is "UOT March II". It has four in-wheel motors and can be controlled independently to improve EV motion behaviors [1].

Figure 1: "UOT March II" and in wheel motors

Since the application of the advantages of electrical motors for EV control systems, not only

conventional control methods can be implemented more easily, but also some advanced control methods which are impossible for ICV can be realized for EV. Therefore the behavior of vehicle might be controlled much well than before. It is one of merits of EV [1][2].

By optimum force control of motored wheels, traction forces between tire and road could be generated. Due to such precise traction force generation, yaw moment, which effects EV yaw rate, can be controlled exactly [3]. In this paper, we will use this kind of yaw moment control strategy to control yaw rate and improve maneuverability and keep safety of EV, even in the case of acceleration or deceleration cornering.

Generally speaking, the yaw moment, which is required for vehicle yaw rate control, could be obtained by force control of only two motored wheels on the different sides of EV. However, if all four wheels of an EV are motored, the same yaw moment value may be obtained by force control of different groups of motored wheels. Therefore, there are some redundant actuators for yaw moment generation.

As for EV control system, that actuator redundancy means the number of control inputs is larger than the number of control outputs. For example, as mentioned above, if we would control yaw rate by using yaw moment which is generated by force control of motored wheels, the control inputs would be force commands to four motors and the control output would be yaw rate. There are four control inputs and one control output. There are two redundant motors in this case.

However, when EV drives in critical or dangerous road conditions, the redundant motors can be used to choose optimum control inputs for avoiding tire slip or wheel lock and keeping stability of EV. In other case, for example, when one motored wheel fails suddenly, the redundant actuators could be used to compensate the failed one and reconfigure the control system. We will deal with that redundancy problem in the section of optimum force distribution.

For using the advantages of redundancy, the information of tire forces should be well known. Although many kinds of expensive sensors are used, it is difficult to clearly know the tire friction forces in real time. Therefore, in this paper we also propose a disturbance observer based force estimation method, which is another key point in this paper.

The remainder of this paper is organized as follows: section 2 is vehicle dynamic analysis of EV; section 3 discusses yaw rate control for maneuverability improvement; section 4 is estimation of lateral force by disturbance observer; section 5 is optimum force distribution; section 6 is preliminary conclusions and future works.

2 Vehicle dynamic analysis

The EV used to study the proposed control method is a 4 wheel motored electric vehicle (4WD in-wheel-motored EV), which is shown in Figure1. The free body diagram is shown in Figure 2. We assume that the front steering angles are controlled by driver and equal to each other. Four motored wheels can be controlled to drive EV by controllers. In this paper, because we mainly discuss the yaw rate control for maneuverability improvement, therefore, it is natural to only consider the vehicle motion in the horizontal plane. We consider three degrees of freedom: the motion in the longitudinal direction X ; the motion in the lateral direction Y ; yaw motion around the vertical axis Z . We also assume that the steering angle δ_f and side slip angle β are very small. The vehicle dynamics can be expressed by

1. longitudinal dynamics

$$Ma_x = F_{x1} + F_{x2} + F_{x3} + F_{x4} \tag{1}$$

2. lateral dynamics

$$Ma_y = MV(\dot{\beta} + \gamma) = F_{y1} + F_{y2} + F_{y3} + F_{y4} \tag{2}$$

3. yaw motion around the vertical axis

$$J\dot{\gamma} = M_{zx} + M_{zy} = M_z \tag{3}$$

$$M_{zx} = d_f(F_{x2} - F_{x1}) + d_r(F_{x4} - F_{x3}) \tag{4}$$

$$M_{zy} = l_r(F_{x3} + F_{x4}) - l_f(F_{x1} + F_{x2}) \tag{5}$$

Where M is vehicle mass; a_x, a_y are longitudinal and lateral acceleration; γ is yaw rate; β is side slip angle; $d_f(d_r)$ is the front (rear) wheel thread; $l_f(l_r)$ is distance between the center of gravity and the front (rear) axis. V is the velocity of EV. $F_{x1}, F_{x2}, F_{x3}, F_{x4}$ are traction forces of tires. $F_{y1}, F_{y2}, F_{y3}, F_{y4}$ are lateral forces of tires. The positions of those forces are shown in Figure 2.

2.1 Linear vehicle model for control design

We assume that lateral tire forces are linear. The linear tire model is used and lateral forces are as follows:

$$F_{yi} = -C_i \alpha_i; i = \{1,2,3,4\} \tag{6}$$

where C_i is cornering power of corresponding tire. α_i is slip angle of each tire. We simplify those variables as

$$C_1 = C_2 = C_f; C_3 = C_4 = C_r$$

$$\alpha_f = \beta - \delta_f + \frac{l_f}{V}\gamma; \alpha_r = \beta - \frac{l_r}{V}\gamma;$$

In this paper, we also assume that the steering angle is small and the longitudinal velocity is constant. As for lateral dynamics of EV, we use steering angle as one input, which is controlled by driver. The other is yaw moment M_{zx}, which is generated by traction forces of each tire.

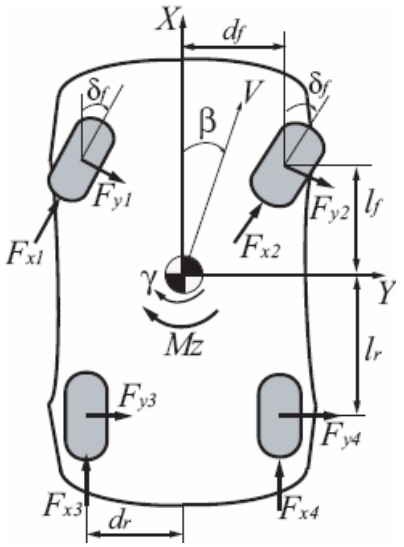

Figure 2: Free body diagram of "UOT March II"

From Eq.1 to Eq.6, we get the linear dynamic model as follow

$$\begin{pmatrix} \dot{\beta} \\ \dot{\gamma} \end{pmatrix} = \begin{bmatrix} -2\frac{C_f + C_r}{MV} & -1 - 2\frac{l_f C_f - l_r C_r}{MV^2} \\ -2\frac{l_f C_f - l_r C_r}{J} & -2\frac{l^2{}_f C_f + l^2{}_r C_r}{J} \end{bmatrix} \begin{pmatrix} \beta \\ \gamma \end{pmatrix} + \begin{bmatrix} 2\frac{C_{fr}}{MV} & 0 \\ 2\frac{l_f C_f}{J} & \frac{1}{J} \end{bmatrix} \begin{pmatrix} \delta_f \\ M_{zx} \end{pmatrix} \tag{7}$$

From Eq.7 we obtain the transfer functions from steering angle and yaw moment to yaw rate as follow

$$\gamma = \frac{G_r(1+T_r s)}{1 + \frac{2\varsigma_n}{\omega_n} s + \frac{1}{\omega^2{}_n} s^2} \delta_f + \frac{G_m(1+T_m s)}{1 + \frac{2\varsigma_n}{\omega_n} s + \frac{1}{\omega^2{}_n} s^2} M_{zx} \tag{8}$$

where G_r, G_m are steady gains. T_r, T_m are time constants. They are all defined according to the vehicle structure parameters [3]. ς_n is the damping coefficient. ω_n is the natural frequency of control system.

As the preparation for next section, we define a reference model according to Eq.7 and Eq.8. We use the same method, which is explained in [4]. According to Eq.8, we choose a reference model which has quick response of yaw rate. The reference model is

$$\gamma^* = \frac{G_r(1+T_r s)}{1 + \frac{2\varsigma_n}{\omega'_n} s + \frac{1}{\omega'^2{}_n} s^2} \delta_f \tag{9}$$

where $\omega'_n > \omega_n$. In this study we define $\omega'_n = 1.5\omega_n$.

3 Yaw rate control for maneuverability improvement

During critical cornering, for example, accelerating or decelerating cornering, yaw rate control is expected to help driver to maintain stability of the vehicle, especially when the driver may have

difficulties or unable to control vehicle by using the steer wheel alone. The objective is to be realized by yaw moment control, which is discussed in the introduction. For the purpose of control robust, we here also use model following control method to control the yaw rate follow the reference yaw rate trajectory, which is defined in Eq.9 and often looked on as a yaw response of vehicle in a case of desired yaw motion.

In this paper we try yaw moment control which is the same as [4]. As Figure 3 shows, yaw moment controller works as the higher controller in whole of our control strategy. It is used to calculate yaw moment, which is the required control quantity for yaw rate stability. This yaw moment controller is designed by "2-DOF" control logic, which integrates yaw rate feed back control with yaw moment feed forward control.

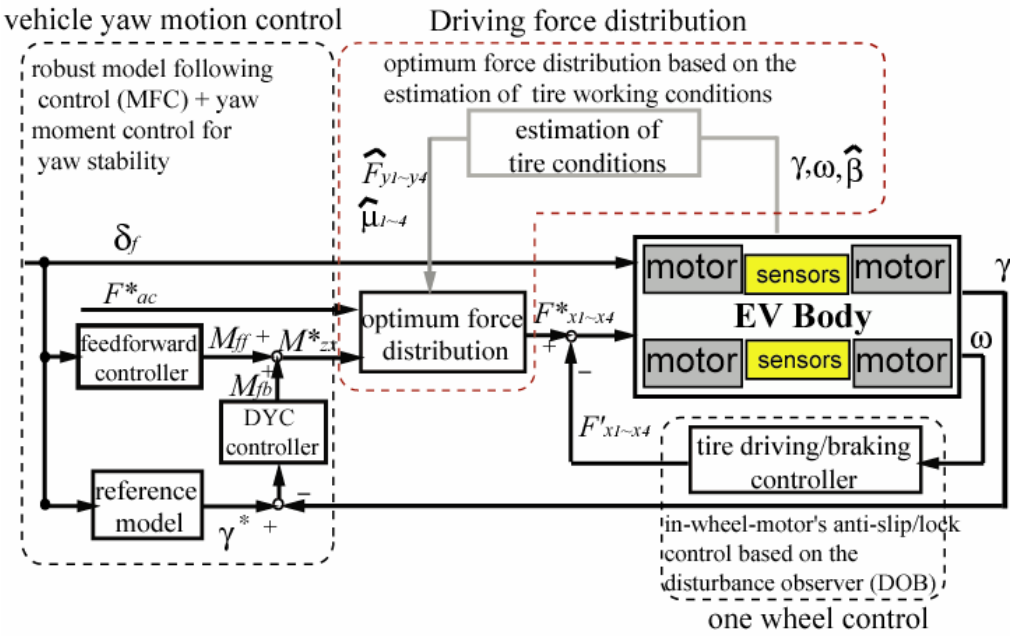

Figure 3: Block diagram of yaw rate control for maneuverability improvement

As mentioned before, the required yaw moment for yaw rate stability should be realized by traction/brake force control of motored wheels. However, from the Figure 3, the quantity of generated yaw moment (M_{zx}^{*}) cannot be looked on as force commands (F_{xi}^{*}) for next minor tire driving/braking controllers. Therefore, as Figure 3 shows, between the higher controller and minor controller, we use the force distribution controller to generate force commands for the minor tire driving/braking force controllers according to the calculated yaw moment M_{zx}^{*}. Further, if in the acceleration or deceleration case, the added driving force commands F_{ac}^{*} should be looked on as another input variable of optimum force distribution, which is also shown in Figure 3.

As the preparation for next section, according to Figure 3, we explain that why estimation of tire force is need for optimum force distribution.

It is well known that the tire friction force has a limitation. If the force control commands (F_{xi}^{*}) are larger than the limitation of tire friction force, tire must slip or lock. And then the EV would be instability. In order to keep the stability of EV maneuverability, we cannot give a control command which is larger than maximum friction force of tire to minor force controller. Therefore the information about tire-road condition, for example, the maximum friction force, is very important for the optimum force distribution [5].

In this paper, we consider tire road friction estimation (TRFE) by using Pacejka tire model based approach which is suggested in [7]. The model is shown in Figure 4. The relationship between the tire slip ratio and road friction coefficient is described based on the brush tire model. In [4] and [5], slop of friction force against slip ratio, which is $\tan\alpha$ and shown in Figure 4, is estimated. By using the

estimated information of slop of friction force against slip, a kalman filter is designed to obtain the maximum value of tire road condition ($\mu_{\max}$).

Considering load transformation because of the acceleration and deceleration, we use the longitudinal acceleration and lateral acceleration to estimate changes of the normal forces F_{zi}. The normal force on the four wheels can be calculated by

$$\hat{F}_{z1} = \frac{Mgl_r}{2l} - \frac{Mh_s}{2l}a_x - k_f\frac{M}{t_f}a_y \tag{10}$$

$$\hat{F}_{z2} = \frac{Mgl_r}{2l} - \frac{Mh_s}{2l}a_x + k_f\frac{M}{t_f}a_y \tag{11}$$

$$\hat{F}_{z3} = \frac{Mgl_f}{2l} + \frac{Mh_s}{2l}a_x - k_r\frac{M}{t_r}a_y \tag{12}$$

$$\hat{F}_{z4} = \frac{Mgl_f}{2l} + \frac{Mh_s}{2l}a_x + k_r\frac{M}{t_r}a_y \tag{13}$$

Second, as for maneuverability improvement, lateral force of tire is also important. Although many kinds of expensive sensors are used, it is difficult to clearly know the tire friction forces in real time. Therefore, we propose a lateral force estimation method which is designed by using disturbance observer.

4 Estimation of lateral force by disturbance observer[7]

4.1 Disturbance observer for traction force estimation

As Figure 5 shows, the dynamics of motored wheel can be expressed by

$$J'_w\frac{d\omega}{dt} = F_m - F_{dis} \tag{14}$$

$$J'_w = \frac{J_w}{r_d} \tag{15}$$

According to Eq.14, longitudinal friction force F_{dis}, which is also called traction force, can be derived by

$$F_{dis} = F_m - J'_w\frac{d\omega}{dt} \tag{16}$$

It is easy to estimate a traction force by using a disturbance observer, which is show in Figure 6.

4.2 Lateral Force estimation based on the disturbance observer

Consider Figure 6, the estimation of traction force of each tire can be used to estimate yaw moment $\hat{M}_{zx}$ which is generated by the left and right tire traction forces. The proposed observer is show in Figure 7.

Rewrite the Eq.2 and Eq.3 as follows,

$$J\frac{d\gamma}{dt} = l_f F_{yf} - l_r F_{yr} + \hat{M}_{zx} \tag{17}$$

$$MV(\dot{\beta}+\gamma) = F_{yf} + F_{yr} \tag{18}$$

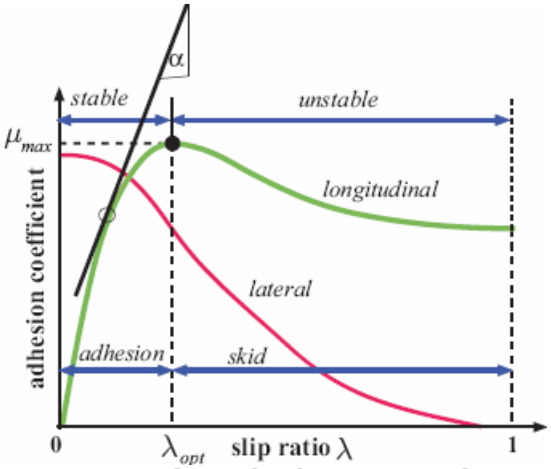

Figure 4: Relationship between tire slip ratio and adhesion coefficient. It is used for estimating road friction condition.

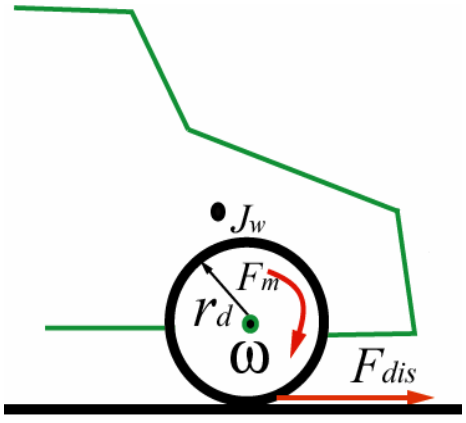

Figure 5: Dynamic of one motored wheel

The front and rear lateral forces can be calculated as follows

$$\hat{F}_{yf} = \frac{1}{l}(l_r MV(\dot{\beta}+\gamma) + J\dot{\gamma} - \hat{M}_{zx}) \tag{20}$$

$$\hat{F}_{yr} = \frac{1}{l}(l_f MV(\dot{\beta}+\gamma) - J\dot{\gamma} + \hat{M}_{zx}) \tag{21}$$

In Eq.20 and Eq.21, deviation of side slip angle $\dot{\beta}$ can be obtained according to the side slip angle estimation, which is expressed in[8]. According to the Eq.7, the derivative variable $\dot{\beta}$ can be expressed by

$$\dot{\beta} = -2\frac{C_f + C_r}{MV}\hat{\beta} + (-1 - 2\frac{l_f C_f - l_r C_r}{MV^2})\gamma + 2\frac{C_{fr}}{MV}\delta_f \tag{22}$$

In this study, we assume that the slip angles and road conditions of left and right tire are equal. We can get the lateral force of each tire as

$$\hat{F}_{y1} = \frac{F_{z1}}{F_{z1}+F_{z2}}\hat{F}_{yf} \tag{23}$$

$$\hat{F}_{y1} = \frac{F_{z1}}{F_{z1}+F_{z2}}\hat{F}_{yf} \tag{24}$$

$$\hat{F}_{y1} = \frac{F_{z1}}{F_{z1}+F_{z2}}\hat{F}_{yf} \tag{25}$$

$$\hat{F}_{y1} = \frac{F_{z1}}{F_{z1}+F_{z2}}\hat{F}_{yf} \tag{26}$$

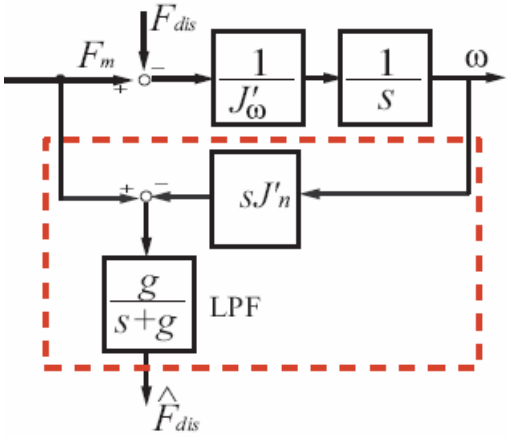

Figure 6: Disturbance observer used for estimating traction force

5 Optimum force distribution

5.1 Objective of optimum force distribution

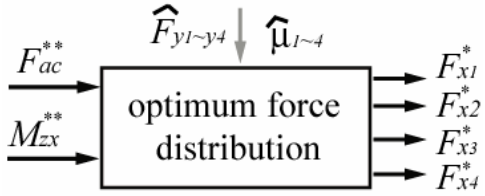

Figure 8: Objective of optimum force distribution

The objective of force distribution in this study, which is shown in Figure 8, is to find suitable force commands for the next force controllers. Then tire traction force will be generated by force control of motored wheels. By the tire traction forces, the target force and yaw moment required for controlling yaw rate of vehicle will be realized.

Force distribution is also a constrained optimal problem. When the control inputs F^{**}_{ac} and M^{*}_{zx} are given, the "optimum finding" should be subject to the following constraints with considering vehicle dynamics.

$$F^{**}_{ac} = F^{*}_{x1} + F^{*}_{x2} + F^{*}_{x3} + F^{*}_{x4} \tag{27}$$

This equation means the sum of the force commands should be equal to the required total accelerating force to meet driver's traction or braking command.

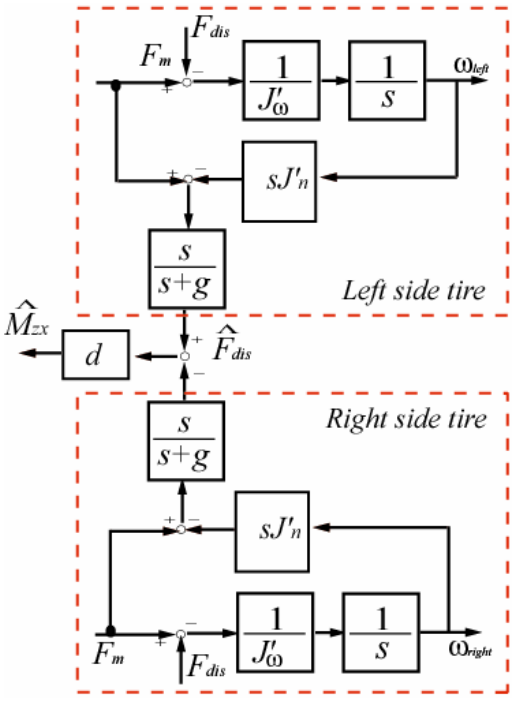

Figure 7: Estimation of yaw moment generated by left and right traction forces

$$M^{**}_{zx} = d_f(F^*_{x2} - F^*_{x1}) + d_r(F^*_{x4} - F^*_{x3}) \tag{28}$$

This equation means yaw moment generated by force commands should be equal to the required yaw moment calculated by higher controller.

$$F^{*2}_{xi} \le \hat{\mu}^2_{\max}\hat{F}^2_{zi} - F^2_{yi}; i \in \{1,2,3,4\} \tag{29}$$

Those inequality equations mean that the generated force commands should be less than the maximum friction force and keep working in the safety domain.

As mentioned in the introduction, there are actuator redundancy problem here. From Eq.28 and Eq.29, two equality constraints are not enough to solve four variables. Hence it is impossible to get unique solutions under such conditions. There are two redundant variables, or we need more constraints conditions to solve force commands uniquely. However, efficient redundancy utilization might bring advantages. For example, it can be used for optimization of some criterion. The tire work load can be minimized by actively controlling redundant actuators. Another example is redundancy control can be used to improve the reliability of EV. Even though one or two motored wheels break down, the control system can still drive EV normally as long as the number of left motored wheels is enough to keep controllable.

As a common idea, the force distribution with redundancy is also looked on as a constraint optimal problem. In the case of this study, one cost function J is chosen to satisfy

$$J(F^*xi) \quad \rightarrow \quad \min$$

Subject to

- Equality constraints: 27,28
- In equality constraints: 29

5.1 Optimum force distribution based on the least square method

Consider that

$$\mu_i^*(F_{xi}) = \frac{F^2_{xi} + \hat{F}^2_{yi}}{\hat{F}_{zi}} \tag{30}$$

We assume that the vector is $u^* = \begin{pmatrix}\mu^*_1 & \mu^*_2 & \mu^*_3 & \mu^*_4\end{pmatrix}^T$. W is a weighting matrix. The cost function is

$$J = \left\| Wu^* \right\|_2^2 \tag{31}$$

Subject to

Subject to

- Equality constraints: 27,28

It is a typical pseudo-inverse problem and can be solved by

$$F^* = W^{-1}(B_v W^{-1})^{\downarrow} \begin{pmatrix} F^{**}_{ac} \\ M^{**}_{zx} \end{pmatrix} \tag{32}$$

where $F^* = \begin{pmatrix}F^*_{x1}, & F^*_{x2}, & F^*_{z3}, & F^*_{z4}\end{pmatrix}^T$, $B_v = \begin{pmatrix}d_f, & -d_f, & d_r, & -d_r\end{pmatrix}$. $()^{\downarrow}$ means the pseudo-inverse.

In fact the optimal results of Eq.32 only considered the effect of load transfer among four motored wheels. It only use load transfer as the force distribution ratio. However, it does not consider the effect of tire lateral force. Further it also does not consider the tire friction force limitation. Therefore, this method should be used in the cases:

- No wheels slip and no wheel slip
- Side slip angle is small and hence the side forces have less effect
- Target force and required yaw moment are not so large and can be realized in no slip domain.

5.2 Optimum force distribution based on the minimax method [9]

Based on the discussion of last subsection, we know that the LSM does not consider the effects of lateral force. However, when EV corners, lateral force will be important to maneuverability.

The minimax method choose the cost function as

$J = \max(\mu^*_i)$

The optimum force distribution can be implemented by

$J \rightarrow \min$

In order to simplify the problem, we reduce the redundancy by distribute left side and right side separately. The minimax is implemented by solve

$$\max\left(\frac{F^{*2}_{x1} + \hat{F}^2_{y1}}{\hat{F}^2_{z1}}, \frac{(F_L^{**} - F^*_{x1})^2 + \hat{F}^2_{y3}}{\hat{F}^2_{z3}}\right) \tag{33}$$

$$\max\left(\frac{F^{*2}_{x2} + \hat{F}^2_{y2}}{\hat{F}^2_{z2}}, \frac{(F_R^{**} - F^*_{x2})^2 + \hat{F}^2_{y4}}{\hat{F}^2_{z4}}\right)$$

The results can be expressed by follows.

$$F_{x1} = \frac{-B_L + \sqrt{B_L^2 - 4A_L C_L}}{2A_L};$$

where $A_L = \frac{1}{\hat{F}^2_{z1}} - \frac{1}{\hat{F}^2_{z3}}$, $B_L = \frac{-2F_L^{**}}{\hat{F}^2_{z3}}$, $C_L = \frac{\hat{F}^2_{y1}}{\hat{F}^2_{z1}} - \frac{F^2{}_L^{**} + \hat{F}^2_{y3}}{\hat{F}^2_{z3}}$

5.3 Simulation results

The simulations are implemented to verify the proposed methods. The input signals are steering angle and driving force. We assume that the friction force coefficient is 0.5. The initial velocity of car is 25 km/m. We also assume that the normal force and lateral force can be estimated by proposed method. Figure 9 shows the yaw rate control results. Figure 10 shows phase-plane curve, which is

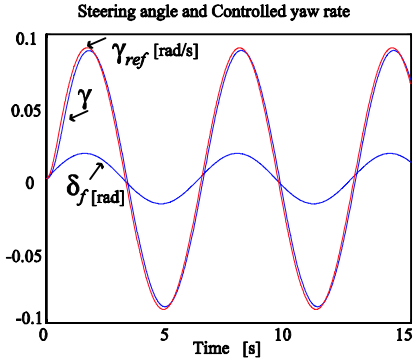

Figure 9: Result of yaw motion control

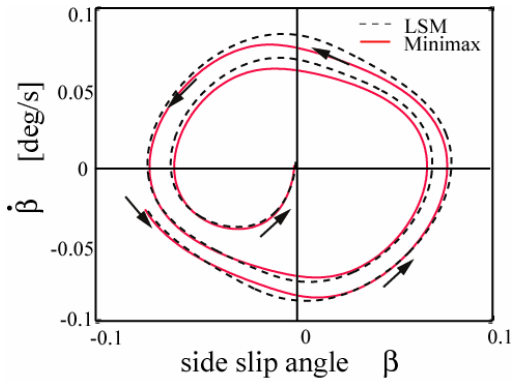

Figure 10: Side slip angle Vs. velocity of slip

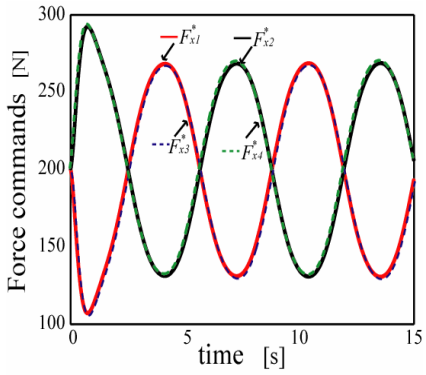

Figure 11: Driving force commands calculated by LSM

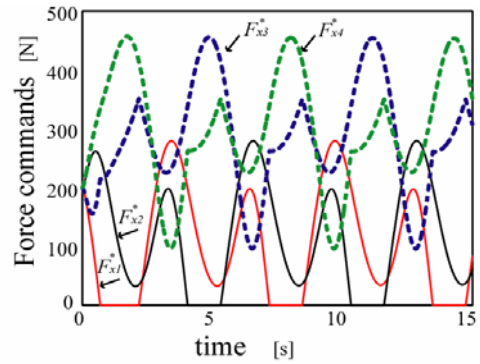

Figure 12: Driving force commands calculated by minimax method

obtained by side slip angle to its velocity. Figure 11 and Figure 12 show the calculating force commands by LSM and minimax method. From that result, the minimax method considers the lateral force of each tire to distribute traction force. LSM does not consider lateral force when distribute traction force. Therefore, Figure 11 shows that the left and right force commands are equal. However, when there is no tire slip, the tire load ratios are almost equal to each other.

When EV drives in a critical case, tire load ratio and the calculated driving force are shown in Figure 15 and Figure 16. At this case, it can be seen that minimax is more stability for yaw rate control.

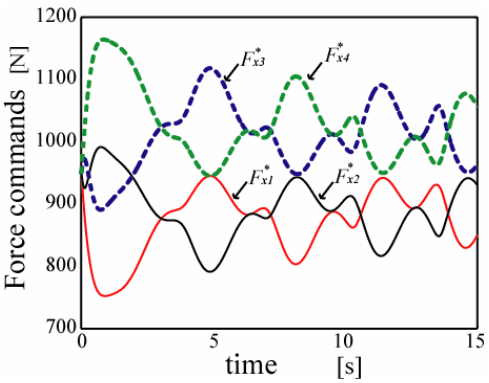

Figure 13: Driving force commands (Minimax)

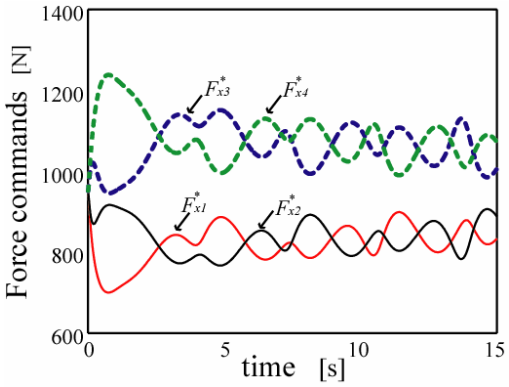

Figure 14: Driving force commands (LSM)

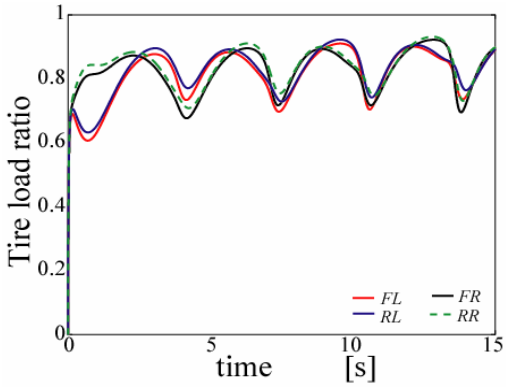

Figure 15: Tire load ratio (Minimax)

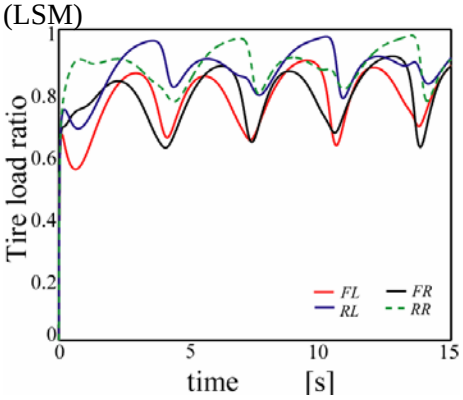

Figure 16: Tire load ratio (LSM)

The generated tire load ratio in Minimax case is less than LSM case.

6 Conclusions and Future works

In this paper we discussed the key point of optimum traction force distribution. Optimum traction force distribution control take full advantage of redundancy. We also discuss disturbance observer based lateral force estimation in this paper.

For the future works, the control strategy should be refined and examined by more experiments. The singularity problems of optimal dynamic redundancy resolution need to be discussed.

References

[1]Yoichi Hori, "*Future Vehicle driven by Electricity and Control Research on 4 Wheel Motored 'UOT March II',"* IEEE Transactions on Industrial Electronics, Vol. 51, No. 5, pp. 954–962, 2004.10.

[2]Shin Ichiro Sakai, Hideo Sado and Yoichi Hori, "*Motion control in an electric vehicle with 4 independently driven in-wheel motors," IEEE Trans. on Mechatronics*, Vol. 4, No. 1, pp. 9–16, 1999.

[3]Peng He, Yoichi Hori, "*Resolving Actuator Redundancy for 4WD Electric Vehicle by Sequential Quadratic Optimum Method," the 19th Japan Industry Applications Society Conference*, Fukui, Japan, 2005.8.

[4]Peng He, Yoichi Hori, Makoto Kamachi, Kevin Walters and Hiroaki Yoshida, "*Future Motion Control to be Realized by In-wheel Motored Electric Vehicle," the 31st Annual Conference of the IEEE Industrial Electronics Society*, Raleigh, North Carolina, USA, 2005. 11.

[5]Hiroshi Fujimoto, Akio Tsumasaka and Toshihiko Noguchi, "*Direct Yaw moment Control of Electric Vehicle*

Based on Cornering Stiffness Estimation," the 31st Annual Conference of the IEEE Industrial Electronics, Society, Raleigh, North Carolina, USA, 2005. 11.
[7]Hideo Sado, Shin Ichiro Sakai and Yoichi Hori, "R*oad condition estimation for traction control in electric vehicle," the* 1999 IEEE international symposium on industrial electrics, bled. Slovenia, 99 TH8465, Vol.2, pp973-978, 1999
[8]Yoshifumi Aoki, Tomoko Inoue, Yoichi Hori, "*Robust design of gain matrix of body slip angle observer for electric vehicle and its experimental demonstration"*, Proceeding of AMC2004, 2004
[9]E.ONO, Y.HATTORI, Y.MURAGISHI and K.KOIBUCHI, "*Vehicle dynamics integrated control for four-wheel-distributed steering and four-wheel-distribution traction/braking system,"* vehicle system dynamics, Vol.44, No.2, February 2006, 139-151

Author

Peng He
Department of Electrical Engineering
The University of Tokyo
4-6-1 Komaba, Meguro, 153-8505
Phone: 0081-3-5452-6289; Fax: 0081-3-5452-6288;
E-mail: ka@horilab.iis.u-tokyo.ac.jp
He received his MS degree in 2001. He is a Ph.D candidate of the University of Tokyo now. His research focuses on robust control, redundancy and optimal control. Now he studies the advanced motion control of electric vehicle.

Yoichi Hori
Institute of Industrial Science
The University of Tokyo
4-6-1 Komaba, Meguro, 153-8505
Phone: 0081-3-5452-6287; Fax: 0081-3-5452-6288;
E-mail: hori@iis.u-tokyo.ac.jp
He received Ph.D degrees in Electrical Engineering from the University of Tokyo in 1983 and joined the Department of Electrical Engineering as a Research Associate. He later became a Professor in 2000. In 2002, he moved to the Institute of Industrial Science as a Professor of Information & Electronics Division. His research fields are control theory and its industrial application to motion control, mechatronics, robotics, electric vehicle, etc. He worked as Treasurer of IEEE Japan Council and Tokyo Section during 2001-2002. He is now an AdCom member of IEEE-IES. He was the Vice President of IEE-Japan IAS in 2004-2005. He has been the chairman of ECaSS Forum since 2005. He is the program chairperson of EVS-22. He is IEEE Fellow.